Electronics Letters, Volume 52, Issue 3, February 2016, pp. 226-228
DOI: 10.1049/el.2015.3907

Experimental Analysis of Multistatic Wind Turbine Radar Clutter Statistics

F. Fioranelli, M. Ritchie, A.Balleri and H. Griffiths

This letter presents preliminary results of the analysis of amplitude statistics of wind turbine clutter as extracted from multistatic radar data. It is shown that the T Location-Scale distribution provides good fitting of the experimental data, and that there are combinations of bistatic angle and polarizations where the bistatic clutter has more favourable statistics for target detection than the simultaneous monostatic clutter.

Introduction: The generation of electricity from renewable sources is a key priority of the United Kingdom and many other countries, and onshore and offshore wind energy is expected to provide a great contribution for this purpose. It has been reported that a single 2.5 MW turbine can generate enough electricity to power 1400 households in a year, which is equivalent to running an average computer for over 2000 years, or making 230 million cups of tea [1].

However, it is well known that wind farms can negatively affect radar systems such as those for Air Traffic Control, air defence and surveillance, and weather forecast. These negative effects include the increase of undesired returns that may generate false alarms, the reduction of probability of target detection in the area above and around wind farms (desensitisation of the radar), and the consequent loss of plotting and tracking capabilities in the affected area [2]. Different mitigation techniques have been proposed in the literature, such as partial reshaping of the turbine with integration of radar absorbing material [3], radically novel wind turbine design [4], and improved digital signal processing algorithms [5] among others. Numerical simulations [6] and controlled laboratory measurements with scaled models of turbines [7] have also been widely investigated to characterize wind turbine clutter in different conditions. A comprehensive campaign to record monostatic Radar Cross Section (RCS) and Doppler signatures at different radar frequency bands was reported in [8-9], but in general there is little information published on actual radar experiments with operational wind farms, especially involving bistatic and multistatic radar. These systems have been mentioned as a possible mitigation approach for wind farm clutter, as multiple views on the area under surveillance as well as different deployment geometries can be beneficial to reduce the adverse clutter effects. In our previous work in [10-11] preliminary results were presented in terms of micro-Doppler signatures of wind turbines extracted from bistatic radar data, with limited bistatic angle of approximately 6.5°.

This letter presents novel preliminary results from a new set of multistatic data with wider bistatic angles up to 23°. The amplitude statistics of wind turbine returns are investigated with fittings of different distributions, in order to compare simultaneous monostatic and bistatic clutter as a function of bistatic angle and different polarizations, namely VV and HH (vertical-vertical and horizontal-horizontal). The statistical analysis of different recordings over time allows to take into account the dynamic yaw angle rotation of the turbine due to changes in wind speed and direction. It is shown that there exists combinations of bistatic angles and polarization where the clutter statistics appear more favourable for bistatic data than for the simultaneous monostatic data, i.e. the bistatic distributions have shorter tails which are more beneficial for target detection against the clutter background. It is believed that these data and results are significant, as there is a limited amount of papers that discuss statistical models of wind turbine clutter [7, 12], and only using monostatic data rather than bistatic/multistatic.

Radar system and measurement setup: The radar used to collect the data is the multistatic pulsed coherent system NetRAD, developed at University College London in the past few years. NetRAD has three distinct but identical nodes, one of which was used as monostatic transceiver (node 3) and the other two as bistatic receivers (node 1 and 2). For this work the frequency was 2.4 GHz (S-band), the transmitted power 23 dBm, the pulse length and bandwidth of the linear chirp modulating the pulse 0.6 μs and 45 MHz respectively, and the pulse repetition frequency (PRF) 5 kHz. Identical antennas with a 10° x 10° beam-width and a 24 dBi gain were used.

Fig. 1 shows the experimental setup. The experiment took place at the Westmill Wind Farm in Watchfield, near Swindon, in May 2015. This wind farm consists of five 49 m tall wind turbines, each one with three 31 m long blades. Only the two turbines closest to the radar nodes were used as targets, and they are labelled as turbine under test 1 and 2 (TUT1 and TUT2). The NetRAD nodes were separated by 50 m and provided simultaneous monostatic and bistatic data with two different bistatic angles β for each measurement, namely 23° and 13° considering the farthest bistatic node (node 2), and approximately 11.5° and 6.5° considering the nearest bistatic node (node 1).As in Fig. 1, it should be noted that the Cranfield University X-band radar was also deployed for simultaneous collection of multiband data. However only results from the analysis of S-band data are presented in this letter.

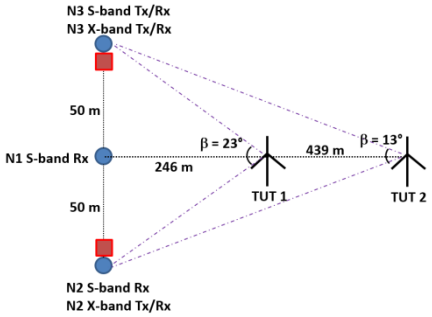

Fig. 1 *Sketch of the experimental setup*

Data analysis: The resolution for the S-band data is sufficient to discriminate in range the return from different turbines, hence the amplitude values at range bins containing the radar echoes from the TUT1 and TUT 2 are analysed separately. These values are related to the RCS of the turbines, but RCS can be properly defined only in the far-field of the turbines, whereas these measurements were performed in the near-field as the far-field distance at S-band would be in the range of 15 km, infeasible in practice for any research radar [7].

Multiple recordings were collected during the day with different polarizations and consecutive recordings were combined together to generate the five datasets analysed in this work. Each datasets include recordings taken over a period of approximately ten minutes with the same transmitted and received polarization, VV or HH. It should be noted that the yaw angle of the turbine with respect to the line of sight of the radar nodes could have changed significantly even in different recordings of the same dataset because of changes in wind direction. Therefore the significant comparison in this analysis is between simultaneous monostatic and bistatic data with different bistatic angles β, rather than between datasets recorded at different times.

The intensity samples of each dataset have been fitted to seven different statistical distributions in order to find the model that presented the best representation of the data. Fig. 2 shows an example of these fittings for both monostatic (node 3) and bistatic (node 2) HH polarised data of the TUT1 returns.

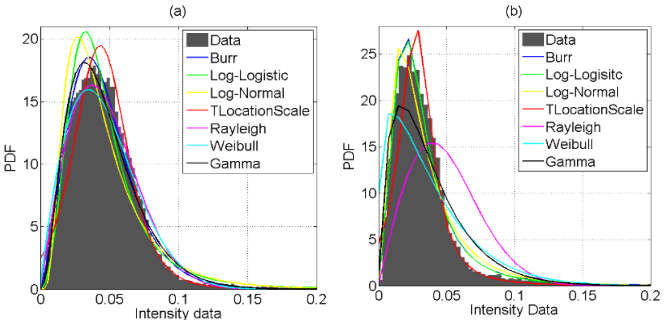

Fig. 2 *Histograms of actual intensity data with 7 PDF distributions fitted to them: (a) monostatic data, and (b) simultaneous bistatic data*

The T Location-Scale provides the best fit, especially for the tail of the distribution, and this appears to be consistent in all the datasets analysed in this work. The probability density function (PDF) of the T Location-Scale is given in (1), where μ is the location parameter (related to the mean value of the samples), σ is the scale parameter (related to the width of the distribution), and υ is the number of degrees of freedom (related to the tail of the distribution, where low values of υ imply heavier and longer tails).

$$f_X(x,\mu,\sigma,\nu) = \frac{\Gamma\left(\frac{\nu+1}{2}\right)}{\sigma\sqrt{\nu\pi}\,\Gamma\left(\frac{\nu}{2}\right)}\left(1+\frac{\left(\frac{x-\mu}{\sigma}\right)^2}{\nu}\right)^{-\frac{\nu+1}{\nu}} \quad (1)$$

The Root Mean Square Error (RMSE) in the log domain between the cumulative distribution function (CDF) of actual data and theoretical distributions was also calculated for a quantitative analysis of the fit. Table 1 shows examples of the RMSE for different nodes and distributions using VV polarised data for the TUT1. The value of RMSE appears to be lower for the T Location-Scale compared with other distributions. These findings agree with those in [12], where such distribution presented a good fitting of experimental data of wind turbine returns. This distribution was fitted to all monostatic and bistatic data using the Maximum Likelihood Estimation (MLE) method, and the fitting parameters are summarised in table 2, showing great variability with polarizations and bistatic angles. Fig. 3 shows comparisons of T Location-Scale distributions fitted to mono and bi data for the TUT1, for both VV and HH polarizations. In both cases the bistatic distribution at node 2 has shorter tail than the monostatic one, which can be beneficial for target detection. This clutter diversity appears to be very dependent on bistatic angles and polarization, hence additional measurements are required to suggest multistatic deployment geometries suitable to mitigate wind farm clutter.

Table 1: Example of RMSE for mono and bi VV polarised data

RMSE	N1	N2	N3
Burr	1.50	1.69	1.36
Log-Logistic	1.41	1.65	1.31
Log-Normal	1.51	1.72	1.41
TLocationScale	1.40	1.53	1.25
Rayleigh	1.76	1.99	1.80
Weibull	1.45	1.64	1.31
Gamma	1.53	1.70	1.41

Table 2: Parameters of the T Location-Scale fitted to the data for different polarizations and different monostatic and bistatic data

Datasets	β	Nodes	Mu	Sigma	Nu
VV TUT1	/	N3	0.039	0.021	4.300
	23°	N2	0.062	0.033	5.472
	13°	N1	0.043	0.023	2.780
VV TUT1	/	N3	0.038	0.023	2.433
	23°	N2	0.037	0.017	2.687
	13°	N1	0.040	0.020	2.457
VV TUT2	/	N3	0.011	0.006	2.583
	11.5°	N2	0.016	0.008	2.836
	6.5°	N1	0.014	0.007	2.607
HH TUT1	/	N3	0.043	0.020	5.090
	23°	N2	0.027	0.013	1.872
	13°	N1	0.049	0.023	2.979
HH TUT2	/	N3	0.011	0.005	3.770
	11.5°	N2	0.012	0.006	2.241
	6.5°	N1	0.016	0.007	2.924

Conclusion: This letter has presented a preliminary analysis of wind turbine clutter amplitude statistics generated from multistatic radar data. It is shown that there are combinations of bistatic angles and polarizations where the bistatic clutter has more favourable statistics for target detection than the simultaneous monostatic clutter. Additional experiments will be performed to gain a better understanding of such clutter diversity.

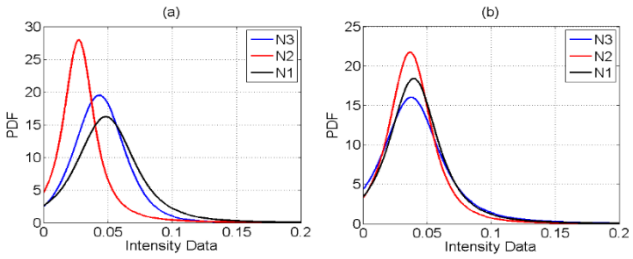

Fig. 3 *Comparison of T-Location-Scale distributions fitted to actual intensity monostatic and bistatic data for (a) HH data and (b) VV data*

Acknowledgments: This work was partially funded by the IET A. F. Harvey Prize awarded to Prof Hugh Griffiths (2013).

F. Fioranelli, M. Ritchie, and H. Griffiths (*Electronic and Electrical Engineering, University College London*)

A. Balleri (*Centre for Electronic Warfare, Cranfield University)*

E-mail: f.fioranelli@ucl.ac.uk

References

1. http://www.renewableuk.com/en/renewable-energy/wind-energy/onshore-wind/index.cfm, Accessed 21/10/2015.
2. C. A. Jackson, "Windfarm characteristics and their effect on radar systems," in *2007 IET International Conference on Radar Systems,* pp. 1-6, 15-18 October, Edinburgh, UK.
3. J. Pinto, J. C. G. Matthews, and G. C. Sarno, "Stealth technology for wind turbines," *IET Radar, Sonar & Navigation*, vol. 4, pp. 126-133, 2010.
4. A. Balleri, A. Al-Armaghany, H. Griffiths, K. Tong, T. Matsuura, T. Karasudani, et al., "Measurements and analysis of the radar signature of a new wind turbine design at X-band," *IET Radar, Sonar & Navigation*, vol. 7, pp. 170-177, 2013.
5. F. Nai, S. Torres, and R. Palmer, "On the mitigation of wind turbine clutter for weather radars using range-Doppler spectral processing," *IET Radar, Sonar & Navigation*, vol. 7, pp. 178-190, 2013.
6. L. R. Danoon and A. K. Brown, "Modeling Methodology for Computing the Radar Cross Section and Doppler Signature of Wind Farms," *IEEE Transactions on Antennas and Propagation*, vol. 61, pp. 5166-5174, 2013.
7. F. Kong, Y. Zhang, and R. D. Palmer, "Wind Turbine Radar Interference Studies by Polarimetric Measurements of a Scaled Model," *IEEE Transactions on Aerospace and Electronic Systems*, vol. 49, pp. 1589-1600, 2013.
8. X. B. M. Kent, K. C. Hill, A. Buterbaugh, G. Zelinski, R. Hawley, L. Cravens, et al., "Dynamic Radar Cross Section and Radar Doppler Measurements of Commercial General Electric Windmill Power Turbines Part 1: Predicted and Measured Radar Signatures," *IEEE Antennas and Propagation Magazine*, vol. 50, pp. 211-219, 2008.
9. Y. A. Buterbaugh, B. M. Kent, K. C. Hill, G. Zelinski, R. Hawley, L. Cravens, et al., "Dynamic Radar Cross Section and Radar Doppler Measurements of Commercial General Electric Windmill Power Turbines Part 2: Predicted and Measured Doppler Signatures," *2007 Antenna Measurements Techniques Association (AMTA) Symposium*, St Louis, MO, USA.
10. M. Ritchie, F. Fioranelli, A. Balleri, and H. D. Griffiths, 'Measurement and analysis of multiband bistatic and monostatic radar signatures of wind turbines', *Electronics Letters*, 2015, v. 51, (14), p. 1112-1113.
11. F. Fioranelli, M. Ritchie, H. Griffiths, and A. Balleri, 'Analysis of Multiband Monostatic and Bistatic Radar Signatures of Wind Turbines', accepted for *2015 Radar Conference*, Oct 2015, Johannesburg, RSA.
12. S. Chiu, 'Wind turbine radar clutter statistics and probability of detection', *2015 IEEE Radar Conference*, pp. 0015-0020, May 2015, Arlington, VA.

Experimental analysis of multistatic wind turbine radar clutter statistics

Fioranelli, Francesco

2023-02-01

Fioranelli F, Ritchie M, Balleri A, Griffiths HD. (2016) Experimental analysis of multistatic wind turbine radar clutter statistics, Electronics Letters, Volume 52, Issue 3, February 2016, pp. 226-228
https://doi.org/10.1049/el.2015.3907